

A SMART PASSIVE YAW DAMPER FOR THE REDUCTION OF LATERAL CONTACT FORCES IN LOW-RADIUS CURVED TRACKS

Gioele Isacchi¹, Francesco Ripamonti¹, Matteo Corsi², Ton van Dongen²

¹Politecnico di Milano
Piazza Leonardo da Vinci, 32 Milano 20133, Italy
gioele.isacchi@polimi.it

²KONI BV
Korteweg 2, 3261 NH Oud-Beijerland, Netherlands
matteo.corsi@itt.com

Keywords: Yaw damper, railway dynamics, curving performance, ripage forces, high-speed railway.

Abstract

High-speed trains are equipped with yaw dampers to prevent the arising of hunting motion. These suspension components play an important role in improving the vehicle stability. However, the presence of yaw dampers increases the steering resistance of the bogies, especially in transient curve track segments. For this reason, passive yaw dampers are designed according to a tradeoff between improvement of high-speed stability and limitation of curving performance degradation. This paper introduces an innovative passive smart yaw damper, the Position Dependent Yaw Damper, able to overcome the typical limitations of standard passive components. The damper can variate its dynamic performances according to the operating conditions of the vehicle. In this paper, a PDYD prototype will be experimentally characterized. Then, a numerical model of the damper will be tuned on the experimental data. The model aims at predicting the influence of the PDYD on the dynamic performances of a rail vehicle, simulated with a Multibody model. A sensitivity analysis will assess the relationship between different PDYD layouts and the vehicle curving performances co-simulating damper and vehicle models. The numerical comparison will be focused on the low-speed negotiation of low radius curves. Finally, the best PDYD layout will be implemented in a numerical simulation of a high-speed high-radius curve to verify its effectiveness in reducing the arising of hunting unstable motion.

1 INTRODUCTION

Nowadays, increasing the commercial speed of railway vehicles is a global trend. This tendency aims at improving the competitiveness of rail transport system respect to other transport categories. For this reason, modern suspension components are designed to allow rail vehicles to reach higher speeds respecting the standard safety and comfort levels [1, 2, 3, 4, 5].

In rail dynamics, the train stability is strongly related to the vehicle speed. In fact, a speed increase may be related to the arising of hunting motion, a typical unstable motion of rail vehicles. Hunting instability is characterized by the coupling of a lateral displacement and a yaw rotation of the

wheelsets. The hunting motion is triggered by the overcoming of a vehicle speed threshold, generally known as critical speed. To reduce the risk of hunting motion, yaw dampers are mounted between car body and bogies in longitudinal direction. They provide an additional energy dissipation which allows the vehicle to reach higher speeds in stable conditions [6, 7]. Although the yaw dampers are fundamental for the stability of high-speed vehicles, they increase the lateral contact forces between wheels and rails. The higher curving resistance of the bogies during the negotiation of sharp curves and switches induces higher wear phenomena at the wheel-rail contact interfaces. Considering that wearing of low radius track segments has a strong relevance in the maintenance expenses of rail networks [8], the standard yaw dampers are designed according to a trade-off between stability and curving performances of the vehicle.

During the last years, several works focused the attention on the design of innovative yaw dampers. In [9], an active yaw damper was designed and tested in field tests, aiming at increasing both stability and curving performances. The implementation of an active yaw damper was also studied in [10] to reduce the guiding forces in small-radius curves. Unfortunately, active solutions require huge efforts in the design of dedicated and expensive solutions with external power supply, control board and different sensors.

In this context, damper manufactures are working on smart passive solution able to autonomously modify their dynamic characteristics. These solutions are designed to be compatible also with old trains and do not require any modification in the vehicle layout. This paper will introduce a passive smart yaw damper, known as Position Dependent Yaw Damper (PDYD). This new device provides a position-dependent damping force as function of the stroke of the device. This paper is organized as follows: in section 2, the damper prototype will be presented and experimentally characterized, comparing its performances with a standard passive device. Then, numerical models of the PDYD and standard yaw dampers will be introduced and implemented on a Multibody model of a rail vehicle. The numerical scenarios simulated to assess the vehicle performances will also be described. Section 3 will report the comparative results between PDYD and standard passive damper, while section 4, discussing the provided results, will conclude the paper.

2 MATERIALS, METHODS AND MODELS

2.1 Position Dependent Yaw Damper

The Position Dependent Yaw Damper (PDYD) has been developed to overcome the typical tradeoff that standard passive dampers must respect. The PDYD can modify its damping force according to the relative stroke of the piston. The damper force is cut by the presence of an additional by-pass channel which is opened when the relative displacement between piston and cylinder overcomes a threshold value. PDYD aims at reducing the damping forces during the negotiation of sharp curves, a working condition characterized by large damper strokes. Rail vehicles run along small radius curves with reduced speed, avoiding the risk of hunting instability. Thus, the force reduction provided by the PDYD during such conditions aims at lowering the lateral contact forces between wheels and rails, reducing the wear phenomena taking place at their interface. The PDYD can autonomously modify its internal characteristics without the aid of any sensor or external power supply.

The PDYD prototype has been manufactured starting from a standard passive yaw damper. An additional by-pass channel has been introduced and designed to be open when the stroke overcomes the cutting position $x_H = 40$ mm. The cutting position is applied symmetrically to reduce the damper force when the stroke is outside the ± 40 mm range. Taking inspiration from the BS EN 13802, an

experimental characterization procedure has been performed on the PDYD and on a standard passive damper. Table 1 reports a selection of three hysteresis cycles that have been imposed on both dampers.

Peak speed [mm/s]	High amplitude cycles		Low amplitude cycles	
	Peak stroke [mm]	Frequency [Hz]	Peak stroke [mm]	Frequency [Hz]
10	50	0.032	2.5	0.637
30	50	0.096	2.5	1.91
100	50	0.318	2.5	6.37

Table 1 Experimental characterization cycles

The characterization tests performed on PDYD aimed at describing the device behavior in both high and low amplitude cycles. High-amplitude low-frequency cycles reproduce the negotiation of sharp curves, while low-amplitude high-frequency cycles simulate the high-speed running of the rail vehicle. Figure 1 reports a comparison of the experimental characterization on both standard passive damper and PDYD. The two devices show similar behavior when dealing with low amplitude cycles, as described in figure 1b. When the damper stroke overcomes the cutting position x_H , the additional by-pass of the PDYD reduces the damping force of the prototype, as shown in figure 1a.

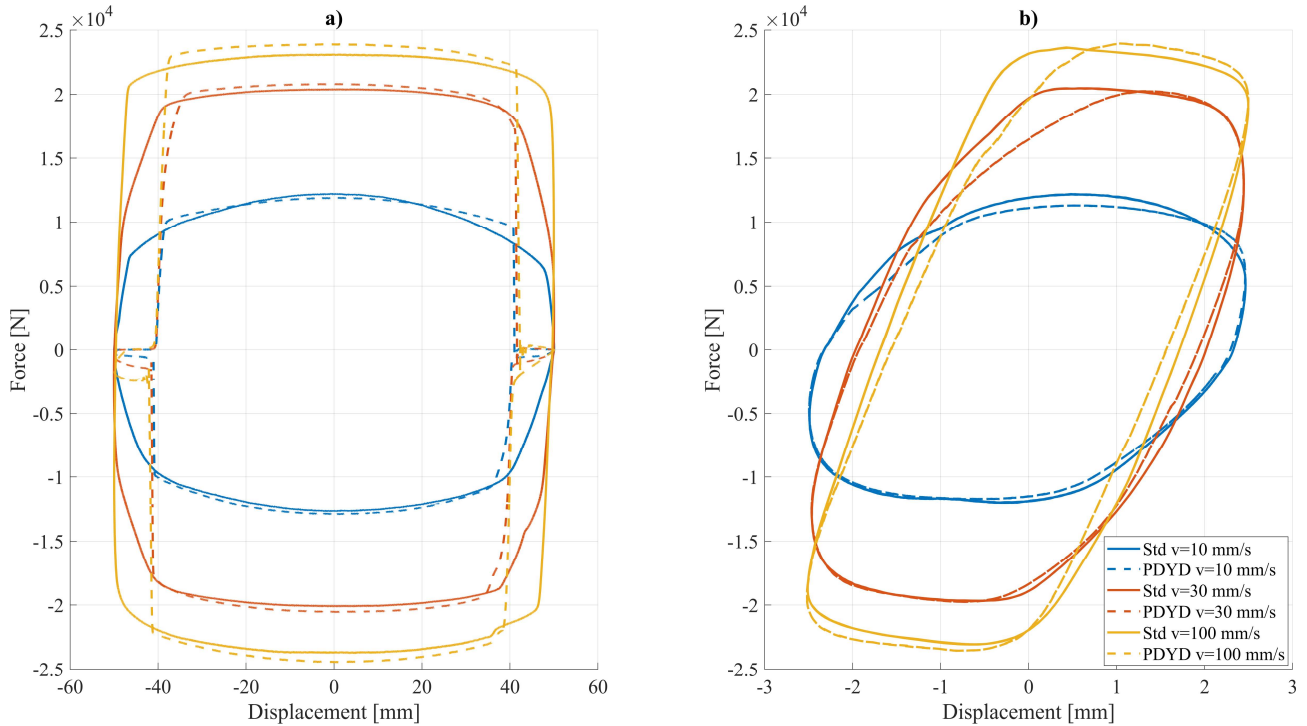


Figure 1 Experimental characterization of standard damper and PDYD: high amplitude cycles (a) and low amplitude cycles (b). The PDYD prototype has been built with a cutting position of 40 mm

The dynamics of PDYD and standard damper has been modelled through a lumped element approach implemented in Matlab/Simulink. Hydraulic dampers are generally defined as dissipative suspension components. Nevertheless, the force provided by these devices has an elastic contribute related to the damper flexibility, whose main contributors are rod stiffness, oil compressibility and the silent-blocks stiffness. Yaw dampers flexibility is fundamental to be consider in railway dynamics due to its strong relevance to vehicle stability [11]. For this reason, an in-series stiffness is considered in the damper numerical models. Within our model, a non-linear asymmetric dashpot and a concentrated mass terms have been considered. The PDYD numerical model presents an exclusive valve modeling able to accounts for the variation of the damping force related to the damper stroke. This feature allows to properly model the effects of the additional by-pass opening of the PDYD. The

parameters of the numerical models have been tuned by simulating the characterization tests of table 1 in virtual environment and comparing numerical and experimental data, as shown in figure 2.

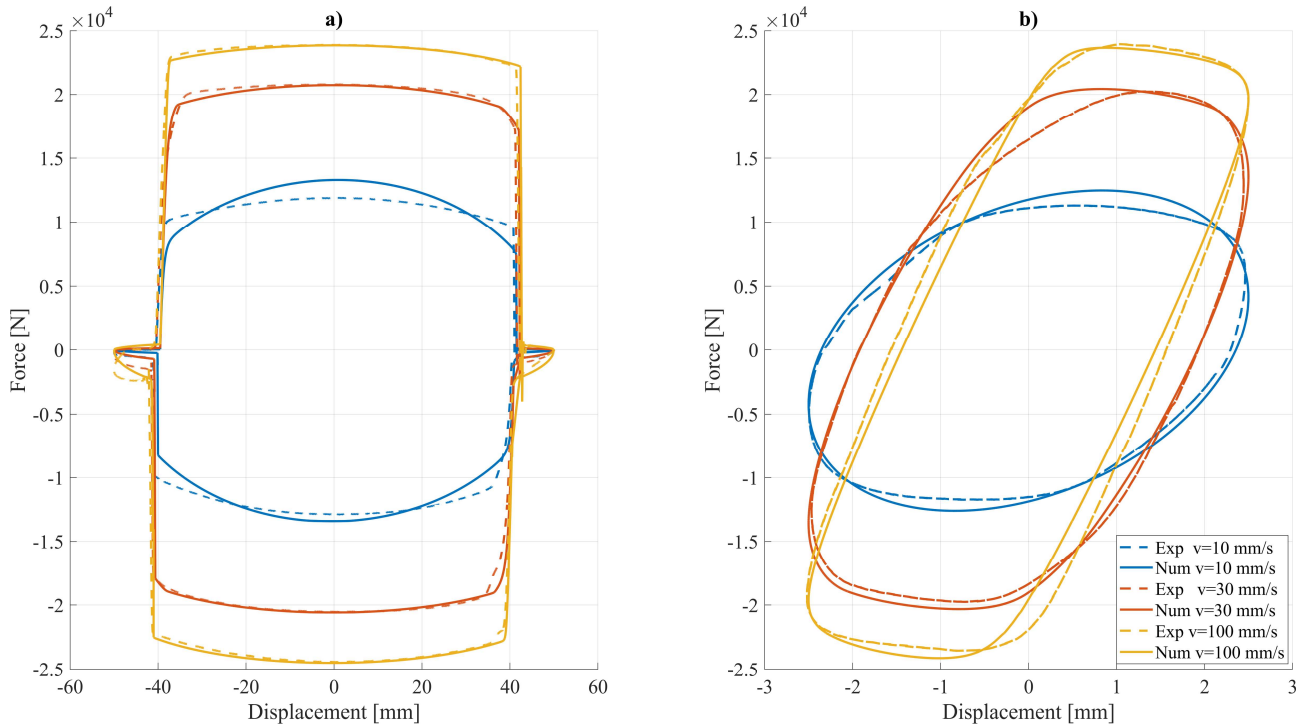


Figure 2 Comparison between numerical and experimental characterization cycles (PDYD)

2.2 Multibody vehicle modeling

The damper numerical models are designed to be co-simulated with in a Multibody environment. The Multibody model of a rail vehicle has been designed to evaluate the effect of different yaw damper solutions on its dynamic performances. The commercial software Simpack has been selected to simulate a test case vehicle equipped with four yaw dampers. The main features of the rail vehicle are reported in table 2. The yaw dampers are modelled through a co-simulation routine. For each time step of the simulation, the Multibody model sends to the damper numerical models a stroke value. The yaw damper forces are calculated through the Simulink/Matlab model and sent back to the Multibody model.

Primary longitudinal stiffness	$k_{x,I}$	5.516 E07 N/m
Primary lateral stiffness	$k_{y,I}$	1.316 E07 N/m
Primary vertical stiffness	$k_{z,I}$	9.700 E05 N/m
Primary longitudinal damping	$r_{x,I}$	5.500 E04 Ns/m
Primary lateral damping	$r_{y,I}$	1.500 E04 Ns/m
Primary vertical damping	$r_{z,I}$	3.200 E04 Ns/m
Secondary longitudinal stiffness	$k_{x,II}$	1.450 E05 N/m
Secondary lateral stiffness (spring)	$k_{y,II}$	1.450 E05 N/m
Secondary lateral bumpstops		Non-linear model
Secondary vertical stiffness	$k_{z,II}$	3.410 E05 N/m
Anti-roll bar stiffness	$k_{\theta,II}$	6.239 E06 N/rad
Yaw dampers		Matlab/Simulink model
Secondary lateral damping		Non-linear model
Secondary vertical damping	$r_{z,II}$	3.0 E04 Ns/m

Wheelset mass	m_w	1873 kg
Bogie mass	m_b	2775 kg
Bogie moment of inertia, x	$I_{xx,b}$	2015 kgm ²
Bogie moment of inertia, y	$I_{yy,b}$	1664 kgm ²
Bogie moment of inertia, z	$I_{zz,b}$	3479 kgm ²
Car-body mass	m_c	3.645 E04 kg
Car-body moment of inertia, x	$I_{xx,c}$	5.973 E04 kgm ²
Car-body moment of inertia, y	$I_{yy,c}$	1.712 E06 kgm ²
Car-body moment of inertia, z	$I_{zz,c}$	1.712 E06 kgm ²

Table 2 Multibody model parameters

2.3 Numerical simulations

The curve-taking performances of the vehicle has been quantified by comparing the ripage forces (also known as track shifting forces) during the negotiation of different curved track segments. The simulated scenarios are listed in table 3, in which curvature radius, rail cant and vehicle speed are reported. The lowest curve radius, 190 m, belongs to a simulation focused on the switch negotiation with null rail cant. The curves 1-8 are characterized by a constant curvature segment between two transient sigmoid segments (curve entry and exit). Both vertical and lateral rail irregularities have been added to the rail track, considering the analytical expressions of their Power Spectral Density provided in [12].

	Curve radius [m]	Rail cant [m]	Vehicle Speed [m/s]
Switch simulation	190	0	12
Curve 1	250	0.028	14
Curve 2	300	0.039	16
Curve 3	350	0.05	18
Curve 4	400	0.061	20
Curve 5	500	0.084	24
Curve 6	600	0.081	26
Curve 7	700	0.080	28
Curve 8	800	0.093	30

Table 3 Track segments simulated with the Multibody model

The influence of the PDYD on the dynamic performances of the rail vehicle is strongly related to its cutting position x_{TH} . When the damper stroke overcomes this threshold, the opening of the additional by-pass channel dramatically decreases the damping force. Thus, a low threshold value can reduce the damping forces during the negotiation of low radius curves. Nevertheless, the cutting position must respect a minimum value to avoid the decreasing the stabilizing effect of the damper during the high-speed negotiation of large radius curves. For this reason, a sensibility analysis focused on different values of the cutting position x_{TH} has been set up. The numerical model of the damper will be modified to investigate the influence on the rail vehicle dynamics of different by-pass stroke thresholds. The PDYD has been tested with seven different cutting positions x_{TH} : 10 mm, 15 mm, 20 mm, 25 mm, 30 mm, 35 mm and the original 40 mm.

3 RESULTS

3.1 Sensitivity analysis: small and mid-radius curves

The PDYD aims at reducing the ripage forces during the negotiation of sharp curves. For the sake of simplicity but without lack of generality, this work will only report the results related to the

absolute ripage forces of the leading wheelset. To summarize the huge amount of data related to the curving performances of the rail vehicle, the curves have been divided into three sub segments (entry transient, constant curve and exit transient). For each sub segment the average and maximum values of the absolute ripage forces have been reported. Figure 3 compares the ripage forces of the leading wheelset with standard damper, PDYD with both $x_{TH} = 10\text{ mm}$ and PDYD with $x_{TH} = 40\text{ mm}$. Figure 3 also shows the subdivision of a curve segment ($R=400\text{ m}$) into the three sub segments previously presented. As expected, the implementation of a PDYD with a sufficiently small x_{TH} allows the reduction of the ripage force especially during the transient sub segments. The higher relevance of the transient sub segments is expected considering the damping nature of the device. Indeed, the damper axial speed reaches larger values during the curve entries and exits, where the damper stroke is being rapidly modified according to the track geometry. Due to its shortness, the switch segment has not been divided into minor sub-segments.

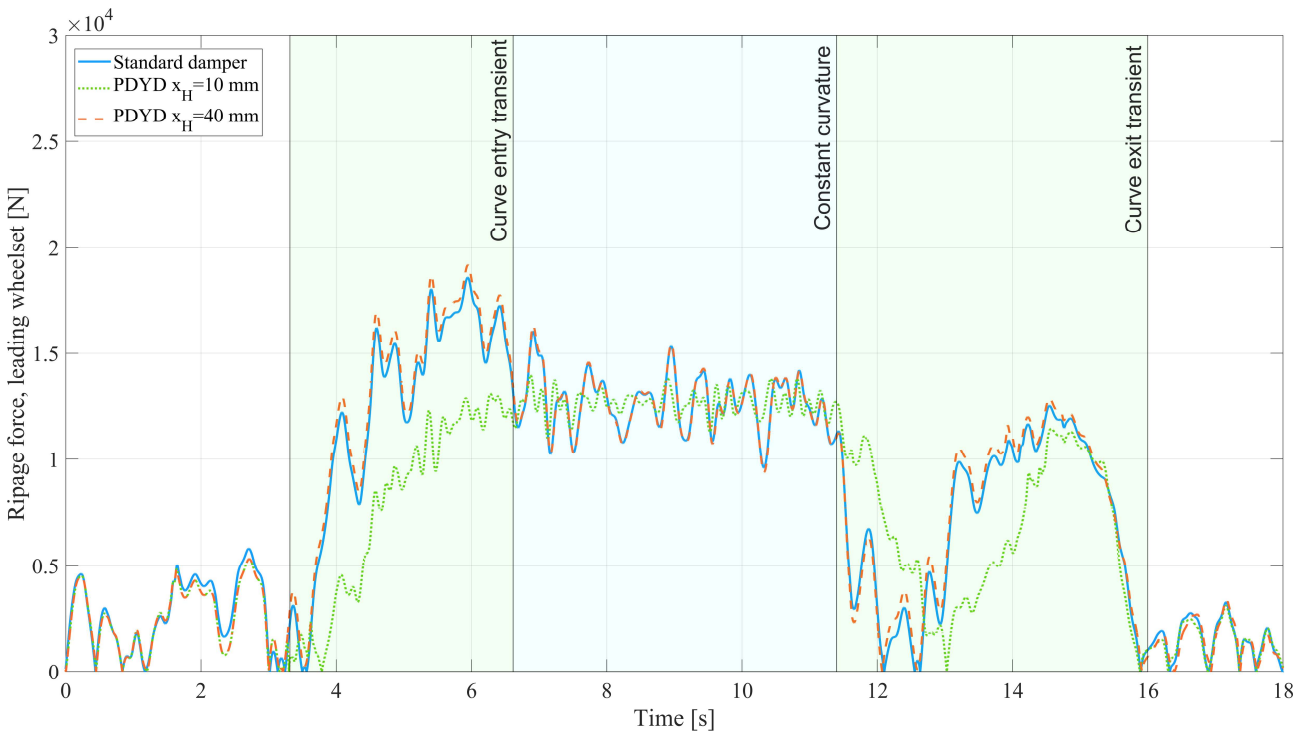


Figure 3 Comparison of the ripage force of the leading wheelset between Standard damper, PDYD with $x_{TH} = 10\text{ mm}$ and PDYD with $x_{TH} = 40\text{ mm}$

The curving performances obtained with the standard damper have been considered as reference. The reduction of ripage forces obtained thanks to the PDYD is correlated to an improvement of the curve-taking behavior in terms of both running safety and reduction of wear phenomena between wheels and rails. Figure 4 reports a summary of the variation of the ripage force average values obtained with PDYD set in different x_{TH} . As expected, PDYD characterized by lower values of x_{TH} increases the curving performance of the vehicle in a wider range of curve radii. In fact, the PDYD with $x_{TH} = 10\text{ mm}$ can provide significant advantages in curves with up to 800 m curvature radius, while higher cutting position values relegate the curving performance improvement only in very sharp curves. The same trend can be observed in figure 5, where the variation of the peak values of the absolute ripage force is reported. The PDYD can reduce the lateral contact forces both in terms of average and peak values.

		Average absolute value of the ripage force of the leading wheelset [N]							
Track segment	Standard Damper	Position Dependent Yaw Damper							
		$x_{TH}=40$ mm	$x_{TH}=35$ mm	$x_{TH}=30$ mm	$x_{TH}=25$ mm	$x_{TH}=20$ mm	$x_{TH}=15$ mm	$x_{TH}=10$ mm	
Switch	21989	-2986	-4013	-4930	-5835	-6694	-7475	-8049	
R=250 m	Entry	12436	610	480	-427	-1615	-2910	-4095	-5277
	Full	18513	-76	-959	-1273	-1312	-1301	-1298	-1301
	Exit	8289	703	1689	2634	3201	3247	2486	1740
R=300 m	Entry	10501	521	522	377	-379	-1649	-2877	-4087
	Full	16819	87	0	-447	-956	-979	-970	-971
	Exit	8197	173	452	1026	1956	2240	1430	766
R=350 m	Entry	7861	197	197	196	-20	-910	-1971	-2825
	Full	14610	91	69	-12	-455	-698	-695	-697
	Exit	7761	152	187	463	924	1391	971	144
R=400 m	Entry	7204	190	190	190	170	-255	-1465	-2569
	Full	13250	80	80	54	-74	-609	-626	-621
	Exit	7694	273	273	371	439	933	737	-354
R=500 m	Entry	5483	70	69	69	69	14	-645	-1402
	Full	10570	54	54	54	50	-57	-501	-502
	Exit	6895	167	167	167	210	363	126	-795
R=600 m	Entry	4018	-59	-59	-59	-58	-59	-305	-782
	Full	5354	33	33	33	33	29	-136	-251
	Exit	6409	180	180	180	181	177	-92	-899
R=700 m	Entry	3713	-54	-54	-54	-55	-54	-68	-145
	Full	2241	71	71	71	71	71	-210	-822
	Exit	6171	137	137	137	137	137	120	-636
R=800 m	Entry	3792	-54	-54	-54	-54	-54	-54	-27
	Full	1823	65	65	65	65	65	48	-627
	Exit	5958	95	95	95	95	95	96	-342

Figure 4 Summary of curving performances: variation of the average value of the absolute ripage force, leading wheelset. Reference value: standard damper

		Maximum absolute value of the ripage force of the leading wheelset [N]							
Track segment	Standard Damper	Position Dependent Yaw Damper							
		$x_{TH}=40$ mm	$x_{TH}=35$ mm	$x_{TH}=30$ mm	$x_{TH}=25$ mm	$x_{TH}=20$ mm	$x_{TH}=15$ mm	$x_{TH}=10$ mm	
Switch	70037	394	-1947	-10131	-6380	-8653	-9896	-8013	
R=250 m	Entry	27940	1081	446	-2929	-6621	-8679	-10853	-10802
	Full	27874	1156	-3138	-9880	-9848	-9856	-9862	-9859
	Exit	17069	-148	96	101	99	102	102	101
R=300 m	Entry	24781	901	901	-1998	-3679	-6170	-9133	-9072
	Full	24985	870	192	-2637	-8191	-8164	-8179	-8169
	Exit	15113	151	166	860	866	865	867	865
R=350 m	Entry	23858	1055	1055	1018	257	-7582	-9409	-9404
	Full	23589	1048	1048	990	-5069	-8589	-8579	-8585
	Exit	13537	458	469	446	489	483	344	327
R=400 m	Entry	18044	655	655	655	656	-1079	-5069	-5300
	Full	18598	588	588	588	-395	-2918	-4606	-4624
	Exit	13509	75	75	435	222	-268	-8	-263
R=500 m	Entry	16558	596	596	596	596	-337	-5881	-5897
	Full	17161	479	479	479	479	-605	-4300	-4283
	Exit	11642	487	483	487	479	535	855	-494
R=600 m	Entry	10917	530	530	539	539	537	-319	-3876
	Full	11742	387	387	387	386	-8	-1774	-3669
	Exit	11713	293	293	293	292	289	330	-24
R=700 m	Entry	8270	432	433	432	433	433	408	-577
	Full	8303	352	352	351	351	351	-711	-3624
	Exit	11054	194	194	194	193	194	198	8
R=800 m	Entry	7763	139	139	140	136	138	137	137
	Full	5752	187	187	187	187	187	510	-2106
	Exit	9644	220	220	220	220	217	229	233

Figure 5 Summary of curving performances: variation of the maximum value of the absolute ripage force, leading wheelset. Reference value: standard damper

3.2 Stability analysis: high speed and high radius curve

Yaw dampers are implemented in railway vehicles to reduce their tendency to show hunting unstable motion. The PDYD with a cutting position $x_{TH} = 10$ mm proved to be able to reduce the lateral contact forces between wheels and rails, thus providing an increase in the curving performance of the vehicle. Nevertheless, a simulation must be performed to verify if the selected stroke threshold is able to avoid unwanted by-pass openings in high-speed running conditions. Due to its position dependent behavior, the most dangerous conditions are related to large radius curve negotiated at high speed. According to [13], the worldwide lowest curve radius in a high-speed rail track, 3200 m, belongs to a curve segment in the French Southeast line, which is negotiated at 270 km/h. A numerical simulation has been set up to compare the stability of the rail vehicle with standard dampers and PDYDs. Vertical and lateral track irregularities have been set similarly to curved track simulations. Figure 6 reports a comparison of the front right yaw damper stroke between standard damper and PDYD with $x_{TH} = 10$ mm. It can be observed that the cutting threshold is high enough to avoid unwanted by-pass openings during this critical high-speed curve. The cutting position of 10 mm has a safety margin which can be estimated around 4 mm. The presence of a safety margin reduces the PDYD sensitivity to geometrical uncertainties that might be related to the manufacturing of the bogie, the car body or the damper itself. This additional analysis excludes the possibility to further decrease the value of the cutting position x_H in PDYD.

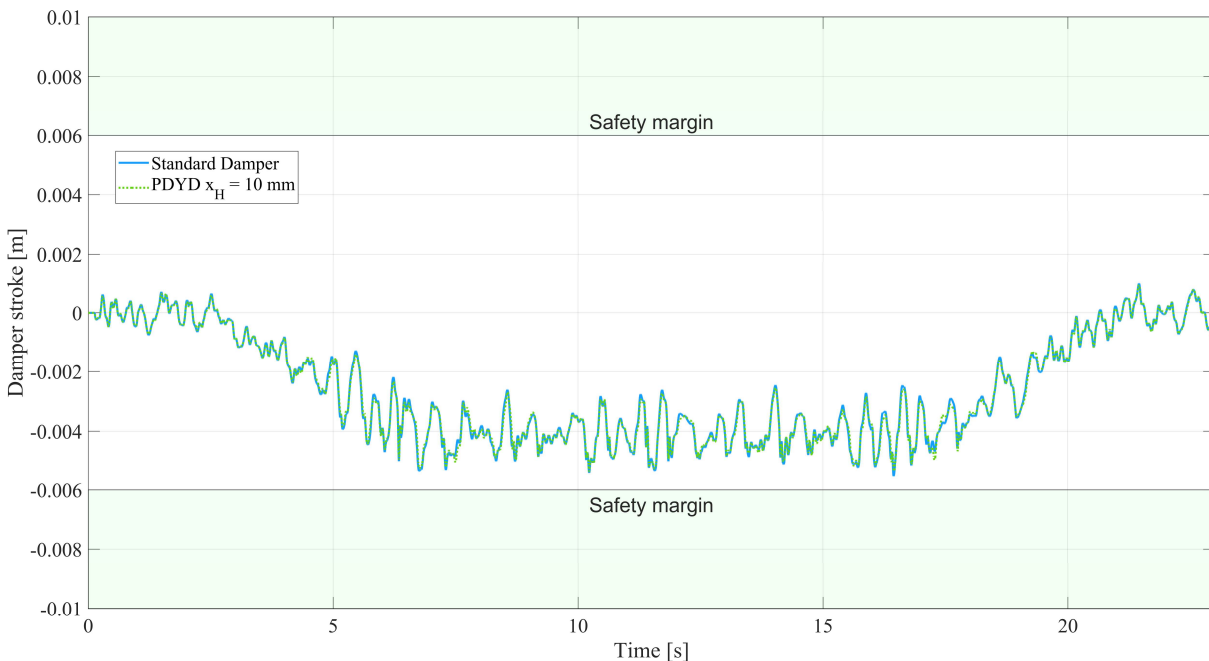


Figure 6 Numerical simulation of a curve with $R=3200$ m negotiated at 270 km/h. Comparison of the front right damper stroke between standard component and PDYD with $x_H = 10$ mm

4 DISCUSSIONS AND CONCLUSIONS

In this work, a smart passive yaw damper, known as Position Dependent Yaw Damper (PDYD), has been introduced. The device aims at reducing the damping forces when the stroke overcomes a specific range, symmetrically defined according to a cutting threshold x_H . The PDYD prototype has been presented and experimentally characterized, comparing its performances with a standard passive damper. Numerical model of the PDYD and standard dampers have been developed and tuned on the experimental data obtained during the characterization tests. The tuned damper models have been

implemented in Matlab/Simulink to be co-simulated with a multibody model of a rail vehicle developed in the commercial software Simpack.

The improvement in the vehicle curving performances obtained thanks to the PDYD have been assessed considering different values of the cutting position x_H . The PDYD layout characterized by $x_{TH} = 10$ mm proved to be the best solution in reducing the absolute ripage forces of the leading wheelset in terms of both average and peak values. The improvement provided by such solution can be observed in curves with curvature radius up to 800 m. The reduction of the average ripage forces reaches absolute variations of up to 8 kN for switch negotiation and 5 kN for low radius curves. The peak value of ripage forces proved to be reduced up to 10 kN. From a relative point of view, the average and peak values reduction can reach the 30% of the performances obtained with standard dampers. The PDYD damper with $x_{TH} = 10$ mm has been tested in a high-speed curve characterized by a radius of 3200 m, the worldwide lowest value in high-speed rail networks. The $x_{TH} = 10$ mm guarantees a stroke safety margin of about 4 mm that avoid the unwanted opening of the by-pass channel during high-speed running, thus eliminating the risk of stability reduction.

In conclusion, the PDYD proved to be an effective solution to alleviate the trade-off between high-speed stability and low-speed curving performances. In fact, the damper can increase the low-speed curving performances of the vehicle without decreasing the running stability in high-speed conditions.

BIBLIOGRAPHY

- [1] F. Ripamonti e A. Chiarabaglio, «A smart solution for improving ride comfort in high-speed railway vehicles,» *Journal of Vibration and Control*, vol. 25, 2019.
- [2] F. Ripamonti, A. Chiarabaglio e F. Resta, «A semi-active damper in vertical secondary suspension for the comfort increase in passenger trains,» in *Proceedings of SPIE - The International Society for Optical Engineering*, 2017.
- [3] R. Corradi, L. Mazzola e F. Ripamonti, «Optimisation of secondary suspension dampers to improve the ride comfort of high-speed rail vehicles,» in *ICSV 2016 - 23rd International Congress on Sound and Vibration: From Ancient to Modern Acoustics*, 2016.
- [4] R. Corradi, L. Mazzola, F. Ripamonti e L. Rosa, «Influence of Underbody Suspended Equipment on Rail Ride Comfort,» in *ASME 2014 12th Biennial Conference on Engineering Systems Design and Analysis*, 2014.
- [5] R. Corradi, S. Melzi, F. Ripamonti e M. Romani, «Estimation of the Comfort Indexes of a Rail Vehicle at Design Stage,» in *ASME 8th Biennial Conference on Engineering Systems Design and Analysis*, 2006.
- [6] A. Alonso, J. Gimenez e E. Gomez, «Yaw damper modelling and its influence on railway dynamic stability,» *Vehicle System Dynamics*, 2011.
- [7] Z. Xia, J. Zhou, D. Gong, W. Sun e Y. Sun, «Theoretical study on the effect of the anti-yaw damper for rail vehicles,» in *Proceedings of the Institution of Mechanical Engineers, Part C: Journal of Mechanical Engineering Science*, 2019.
- [8] A. Nissen, «Classification and cost analysis of switches and crossings for the Swedish railway: a case study,» *Journal of Quality in Maintenance Engineering*, 2009.

- [9] F. Braghin, S. Bruni e F. Resta, «Active yaw damper for the improvement of railway vehicle stability and curving performances: simulations and experimental results,» *Vehicle System Dynamics*, 2006.
- [10] T. Michalek e J. Zelenka, «Reduction of lateral forces between the railway vehicle and the track in small-radius curves by means of active elements,» *Applied and Computational Mechanics*, 2011.
- [11] S. Bruni, J. Vinolas, M. Berg, O. Polach e S. Stichel, «Modelling of suspension components in a rail vehicle dynamics context,» *Vehicle System Dynamics*, 2011.
- [12] *ERRI B176 RPI Bogies with steered or steering wheelsets*, Utrecht.
- [13] Y. Sirong, «Chapter 6 - Calculation Method for Minimum Curve Radius of High-Speed Railways,» in *Dynamic Analysis of High-Speed Railway Alignment*, Academic Press, 2018, pp. 153-199.